http://dx.doi.org/10.21577/0103-5053.20170210

J. Braz. Chem. Soc., Vol. 29, No. 4, 856-872, 2018.
Printed in Brazil - ©2018 Sociedade Brasileira de Química

Article

Theoretical Study of the Interaction of 1,2-Dithiolene Ligands with the Mg^{2+} and Ca^{2+} Aquacations: Electronic, Geometric and Energetic Analysis

Glauber S. Melengate,[a] Stanislav R. Stoyanov,*[,b,c] Daniel G. S. Quattrociocchi,[a] Leonardo M. da Costa*[,d] and Glaucio B. Ferreira*[,a]

[a]*Programa de Pós-Graduação em Química, Departamento de Química Inorgânica, Instituto de Química, Universidade Federal Fluminense, Outeiro de São João Batista s/n, 24020-141 Niterói-RJ, Brazil*

[b]*Natural Resources Canada, CanmetENERGY in Devon, 1 Oil Patch Drive, T9G 1A8 Devon, Alberta, Canada*

[c]*Department of Chemical and Materials Engineering, University of Alberta, T6G 2V4 Edmonton, Alberta, Canada*

[d]*Departamento de Química Orgânica, Instituto de Química, Universidade Federal Fluminense, Outeiro de São João Batista, s/n, 24020-141 Niterói-RJ, Brazil*

The B3LYP/6-311++G(d,p) method is employed to carry out calculations of the interaction strength of bidentate dithiolene ligands with the $[M(H_2O)_6]^{2+}$ and $[M(H_2O)_4]^{2+}$ (M = Mg or Ca) aquacations. Two series of ligands are studied: one with a phenyl ring directly bonded to the S interacting atoms and the other with a substituted ethylene (>C=C<) bonded to the two sulfide groups. These ligands present substituents with distinct induction and resonance electronic donor/acceptor effects. Fundamental characteristics, such as geometry, charges and energy of the complexed aquacations and isolated ligands, are analyzed and rationalized to correlate with the substituents effects and the metal-ligand affinity. The thermodynamic results, energy decomposition analysis (EDA) and natural bond order (NBO) show the chelate effect has an important contribution to complex stabilization and leading to an enhanced knowledge of the metal-dithiolene interaction and coordination affinity between the alkaline earth metals and sulfured ligands.

Keywords: divalent metal cation, Ca^{2+}, Mg^{2+}, dithiolene ligands, EDA, NBO, DFT

Introduction

The complexation of metal cations by 1,2-dithiolene ligands is an important research field of coordination and materials chemistry.[1-4] Homoleptic dithiolene complexes are important precursors of molecular devices,[5] semiconductors for field-effect transistors,[6] near infrared (NIR) dyes for lasers,[7,8] liquid crystal and non-linear optical devices,[9,10] electronic recording disks[11] and in olefin purification systems.[12] In the heteroleptic dithiolene complexes, the metal cation interacts with the dithiolate ligand and also with several other ligands, such as cyclopentadienyl, *ortho*-diimines and diphosphines. These molecules have multiple applications, such as models compounds of enzymes,[13] luminescent properties,[14] photo and thermo-solvatochromism,[15-17] catalyst for molecular hydrogen production[18] and dye-sensitized solar cell.[19] In addition, structural modifications on the ligands, such as the number of sulfur atoms, can change the crystalline arrangement of the system leading to new electronic, optical and magnetic properties.[20] The high thermal and photochemical stability and the intense absorptions near the infrared region are due to the combination of these ligands with the metal cations with enhanced orbital overlap.[21]

The interaction between divalent metal cations and organic ligands was analyzed in a large number of studies.[22-37] The interaction of alkaline earth metal cations with O- and N-coordinating ligands was quantified by binding energies, highest occupied molecular orbital (HOMO) and lowest unoccupied molecular orbital (LUMO) energies and energy gap values as well as metal-ligand bond length, and ligand-to-metal electronic donation. It was seen that the O-coordinating ligands have the largest affinity for those cations.[22] Huang *et al.*[23] studied the structure, bonding nature, and stability of divalent and trivalent

*e-mail: glauciobf@vm.uff.br; lmcosta@id.uff.br; stoyanov@ualberta.ca

metal complexes with O-interacting ligands, where the principal parameter to measure the ligand's affinity for the metal cation was the Gibbs free energy of coordination. Ligands with neighboring electron donor groups have stronger interaction with the metallic center than ligands with electron withdrawing groups. Wolf and Hummel[24] have studied the interaction between dithiolene ligands (as maleonitrile-2,3-dithiolate, mnt) with alkaline earth cations. They reported that the ligands bind preferentially the sulfur and nitrogen atoms. The synthesis of dithiolene compounds complexed (cyclobutene-1,2-dithione-3,4-dithiolate) with alkaline earth metal cations was reported by Becher *et al.*[25,26] They found that the dithiolene ligands bind strongly to the metallic center than the water molecule.

The interaction of the divalent metal cations (Co^{2+}, Ni^{2+}, Cu^{2+}), from the water environment, with divalent ligands (2,4-dichlorophenoxyacetic acids, herbicides) was analyzed by Drzewiecka-Antonik *et al.*[27] It was noted that after the first and second ligand complexation the octahedral interaction geometry was maintained. Xia *et al.*[28] performed a theoretical investigation on electronic structures and stability of palladium and platinum complexes, and obtained structural parameters comparable with the experimental values. The natural bond order (NBO) analysis results showed that the metal-ligand bonding was predominantly ionic in nature and the electrostatic interaction was dominant, with strong donor-acceptor interactions. Plazinski and Drach[29] studied the interaction of amino acid residues with Zn^{2+}, Cd^{2+}, Cu^{2+}, Mn^{2+} and Co^{2+}. These authors determined the preferred binding trends for the coordination with each cation and the affinity order by the calculation of the Gibbs free energy change for the metal complexation. Tavassoli and Fattahi[30] analyzed the interaction between the Zn^{2+}, Ca^{2+} and Mg^{2+} with the histidine ligand. They concluded that the stronger interaction is with the softest transition metal cation due to the larger covalent component of the interaction, even though the electrostatic character is predominant. Yánez *et al*.[34] extensively studied the interaction of metal cations with O-, N- and S-coordinating ligands.[31-34]

Geometrical, electronic and energetic characteristics of the complexes and the isolated ligands were rationalized to explain metal-ligand affinity trends. It was found that the peripheral groups bonded to the anchoring atom that binds to the metal cation modulate the interaction strength. Pesonen *et al.*[35] performed a density functional theory (DFT) study of the interaction of mono- and bidentate ligands with metal cations, where the interaction with the bidentate ligands was stronger than that with monodentate ones. The size of the cation, its softness and the stabilization energy of ligand's chelation directly affected the coordination preferences. The octahedral arrangement was maintained around Mg^{2+} and Ca^{2+} in the first substitution reaction. In the metal-ligand interaction field, Despotovic[36] and Kowalsak-Baron[37] observed that the nature of the interaction was directly influenced by the charges on the interacting atoms, bond length and cation hardness as well as orbital overlap, HOMO-LUMO energy gap, according to NBO and energy decomposition analysis (EDA) results.

These previous studies analyzed geometrical, electronic and energetic parameters of the metal-ligand interaction to help understand the affinity of each class of molecule for the metal cation.[38-47] With the same objective, here we employ the B3LYP functional[48] to analyze the affinity of the Mg^{2+} and Ca^{2+} aquacations for the dithiolene ligands and to rationalize it through correlations with parameters of fundamental chemistry. Moreover, the EDA,[49-51] NBO[52] and donor-acceptor analysis methods are employed to further elucidate the character of the metal-dithiolene coordination interactions.

Methodology

Geometry optimization and energy calculations were carried out using the hybrid B3LYP[53] functional and the 6-311++G(d,p) basis set,[54-57] as implemented in the Gaussian 09 software.[58] Frequency calculations were performed to ensure each optimized structure is a genuine minimum on the potential energy surface and compute the thermochemistry results. The counterpoise procedure was used to calculate the basis set superposition error (BSSE).[59,60] The B3LYP/6-311++G(d,p) method leads to results in agreement with higher level of theory *ab initio* calculations.[61,62] The EDA calculations[49-51] were also performed using the B3LYP/6-311++G(d,p) method, as implemented in the GAMESS software.[63,64] In the EDA procedure, the sum of the electrostatic ($E_{Elec.}$), polarization ($E_{Pol.}$), exchange ($E_{XC.}$), dispersion ($E_{Disp.}$) and Pauli repulsion (E_{Pauli}) components leads to the total interaction energy ($E_{Tot.}$).[49-51] The sum of the polarization and exchange components gives the covalent term. The NBO analysis was performed using the B3LYP/6-311++G(d,p) method as implemented in the FIREFLY (PC-GAMESS)[65,66] software to obtain the percentage contribution of each resonance structure to the final hybrid molecule. We also computed the acid-base interaction between the aquacomplexes and the ligands using the second-order perturbation energy analysis.[67] All the structures were drawn with the Gaussview 5.0 program.[68]

Results and Discussion

Complexes and reactions studied

Two series of dithiolate ligands are studied, one containing a phenyl ring directly bonded to the S interacting atoms (Figures 1a-1c) and the other containing a substituted ethylene group bonded to the two sulfide groups (Figures 1d-1g). Experimental measurements show that the most common coordination number in water solutions for both the Mg^{2+} and Ca^{2+} cations is 6 with an octahedral arrangement.[69,70] In this way, we analyze two substitution reactions for the Mg^{2+} and Ca^{2+} aquacations, according to equations 1 and 2, to determine the energy for substitution of water molecules by a bidentate dithiolene ligand, as shown in Figure 2. Several studies report this methodology to determine the strength of binding of metal cations and ligands.[22-36,38-47]

$$[M(H_2O)_6]^{2+} + L^{2-} \rightarrow [M(H_2O)_4L] + 2\ H_2O \quad (1)$$

$$[M(H_2O)_4L] + L^{2-} \rightarrow [M(H_2O)_2L_2]^{2-} + 2\ H_2O \quad (2)$$

The focus of this study is to rationalize the role of ligand structural modifications, as the insertion of electron donor, acceptor and aromatic groups, in the modulation of the metal-ligand interaction strength. Both EDA[49-51] and NBO analysis[52] methods are employed to elucidate important contributions to the stabilization of the complexes.

Ligand affinity

The geometries of the 14 calcium and 14 magnesium aquacomplexes were fully optimized using the B3LYP\6-311++G(d,p) method. Figures 3 and 4 show the Mg^{2+} and Ca^{2+} aquacomplexes after the first and second substitutions by the dithiolene ligand, respectively. We

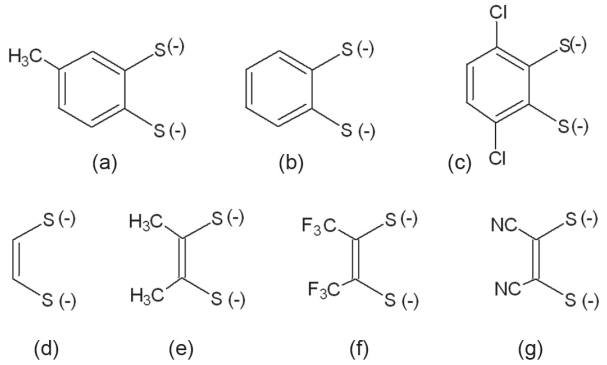

Figure 1. Dithiolene ligands with respective abbreviations: (a) toluene-3,4-dithiolate (tdt); (b) benzene-1,2-dithiolate (bdt); (c) 3,6-dichlorobenzene-1,2-dithiolate (Cl_2-bdt); (d) ethylene-1,2-dithiolate (edt); (e) 1,2-dimethyl-1,2-ethylenedithiolate (mdt); (f) bis(trifluoromethyl) ethylenedithiolate (tfd); (g) maleonitrile-2,3-dithiolate (mnt).

observe that the first ligand substitution did not change the coordination geometry around the metal cation, maintaining the octahedral arrangement, and yielding neutral complexes. However, the second ligand substitution promoted a distortion in the final aquacomplex geometry. We found three distinct coordination geometries for the disubstituted aquacomplexes: octahedral, distorted bipyramidal with trigonal base and tetrahedral. In the tetra and penta coordinated geometries, we observed a withdrawal of water molecules from the coordination sphere that migrate to form a second solvation shell. These water molecules continue to solvate the substituted metallic complex by electrostatic and hydrogen bond interactions with water molecules of the first coordination sphere and with the S atom. The largest distortion in the coordination sphere is obtained for the tetrahedral complex with ethylene-1,2-dithiolate (edt), $[Ca(H_2O)_2(edt)_2]^{2-}$. Table 1 shows the symmetry of each final complex structure after the first and the second ligands substitution. In the second ligand substitution, the complexation of Mg^{2+} with the

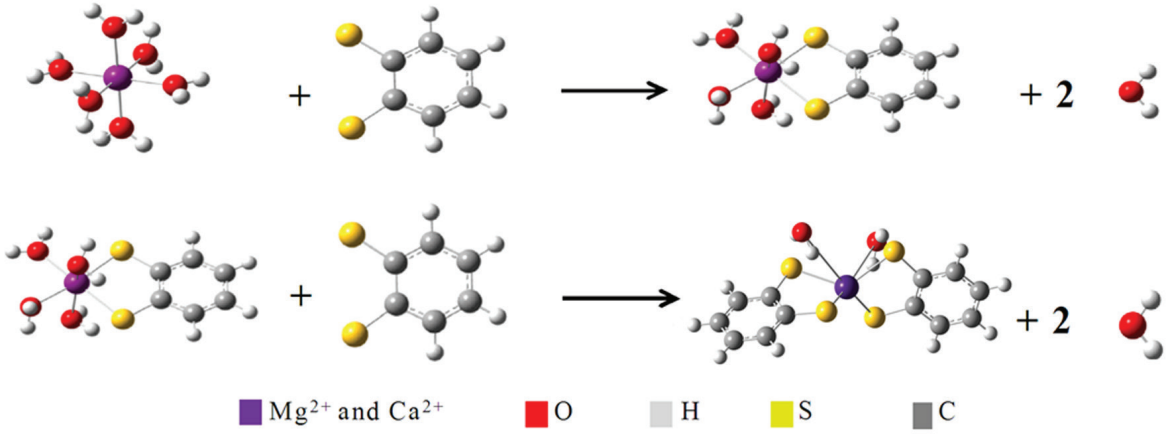

Figure 2. First and second substitution reactions of $[M(H_2O)_6]^{2+}$ and $[M(H_2O)_4L]$ (M = Ca or Mg), respectively, with the bdt dithiolene ligand (L).

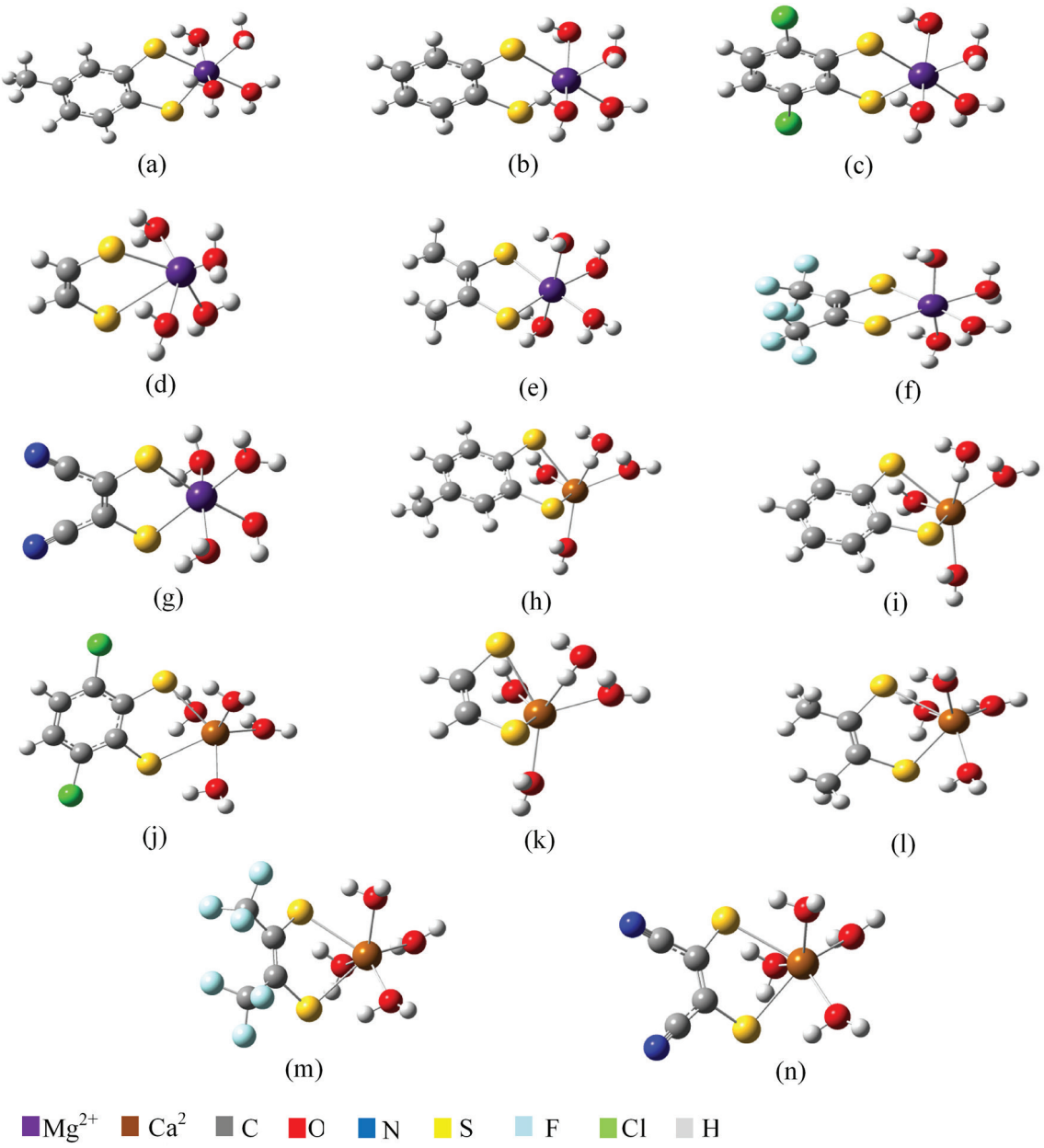

Figure 3. Optimized structures of the monosubstituted aquacomplexes $[Mg(H_2O)_4L]$ and $[Ca(H_2O)_4L]$ containing tdt (a, h), bdt (b, i), Cl_2-bdt (c, j), edt (d, k), mdt (e, l), tfd (f, m) and mnt (g, n) ligands.

toluene-3,4-dithiolate (tdt), benzene-1,2-dithiolate (bdt) and edt leads to a tetrahedral arrangement, the 1,2-dimethyl-1,2-ethylenedithiolate (mdt) presents a bipyramidal structure, whereas 3,6-dichlorobenzene-1,2-dithiolate (Cl_2-bdt), bis(trifluoromethyl) ethylenedithiolate (tfd) and maleonitrile-2,3-dithiolate (mnt) conserved the initial octahedral symmetry. It is interesting to note that on one hand the 3 ligands (Cl_2-bdt, tfd and mnt) with electron withdrawing groups yield complexes with the same symmetry of interaction (octahedral). On the other hand, the ligands (tdt, bdt, edt and mnt) that do not possess electron withdrawing groups present final coordination geometry with a decreased coordination number. This may be due to the ligand charge transfer to the metal center. As Mg^{2+} is a dication, the second substitution by a dianionic ligand causes an increase in the electron density on the metal center, which may promote electronic repulsion between the ligands and saturation of electronic charge on the metal atom. The combination of these two effects may force the migration of weakly-binding ligands, such as neutral water molecules, to the second solvation shell and modify the coordination geometry. For the Ca^{2+} complexes a similar behavior is found. All the monosubstituted $[Ca(H_2O)_4L]$ aquacomplexes maintain the octahedral arrangement. For

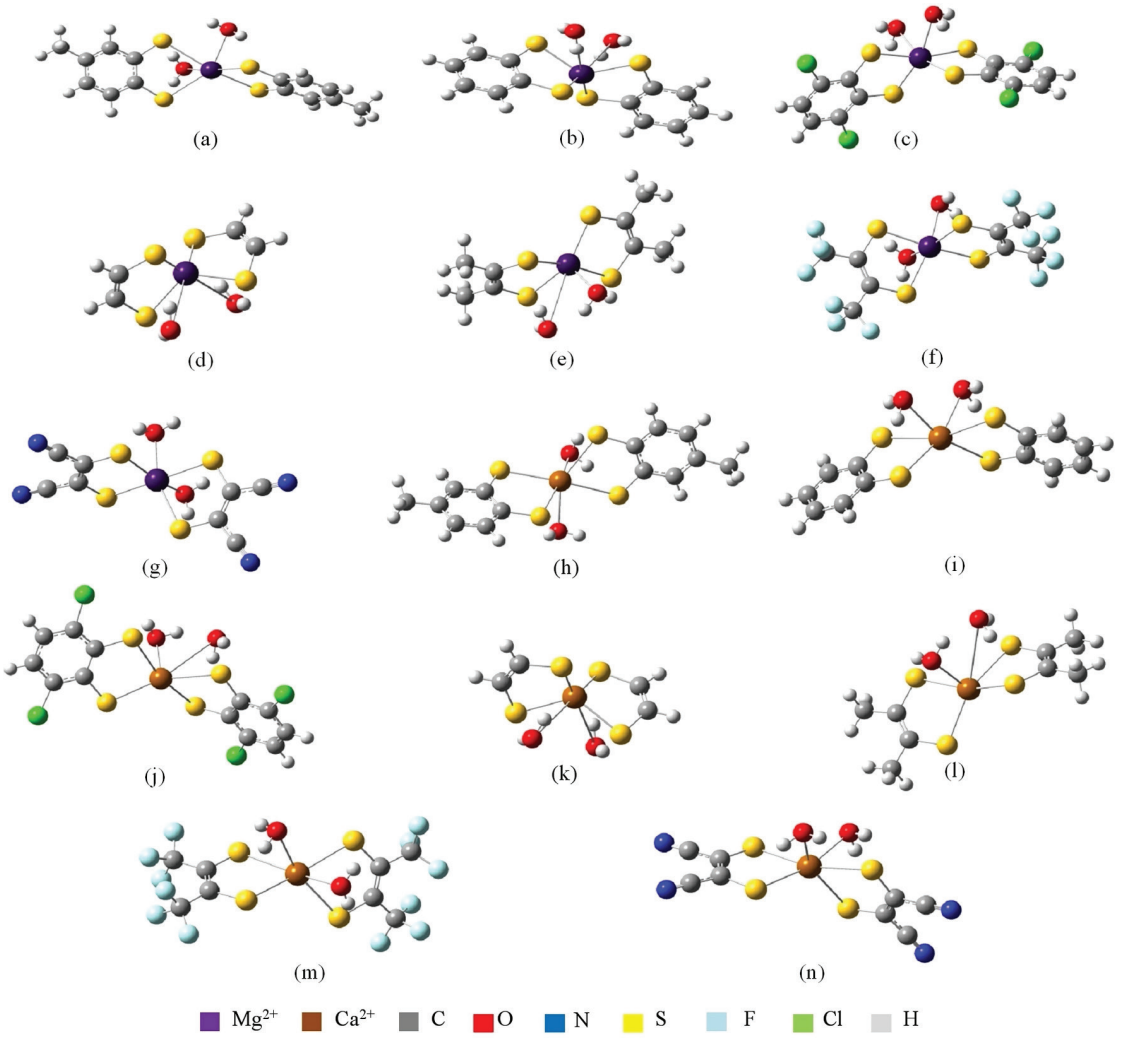

Figure 4. Optimized structures of the disubstituted aquacomplexes $[Mg(H_2O)_2L_2]^{2-}$ and $[Ca(H_2O)_2L_2]^{2-}$ containing tdt (a, h), bdt (b, i), Cl_2-bdt (c, j), edt (d, k), mdt (e, l), tfd (f, m) and mnt (g, n) ligands.

the disubstituted $[Ca(H_2O)_2L_2]^{2-}$ aquacomplexes the tdt, bdt, tfd and mnt ligands maintains the coordination axis with an octahedral, arrangement. The interaction with the Cl_2-bdt, mdt ligands present the bipyramidal final coordination geometry, whereas the edt the tetrahedral optimized geometry. As Ca^{2+} has larger ionic radius (190 pm) than Mg^{2+} (145 pm),[71] it can accommodate more electron density donated from the ligands, as evidenced from the larger number of complexes with octahedral and bipyramidal geometries, the two highest coordination numbers. Additionally, the repulsion between the ligands is larger in the Mg^{2+} aquacomplexes than in the Ca^{2+} derivatives due to the shorter M–L bonds.

The affinity of each ligand for the metal cations was determined from the interaction enthalpy (ΔH) and Gibbs free energy at 298 K (ΔG) for the water exchange by one or two ligand molecules. The affinity results of the ligands for Mg^{2+} and Ca^{2+} are listed in Table 1.

The analysis of Table 1 shows that all the interacting enthalpy values are negative indicating that the substitutions of water molecules for one and two dithiolene ligands are exothermic. Table 1 shows that the second ligand substitution presents less negative interaction enthalpy values than the first substitution by 292.10 and 276.09 kcal mol^{-1} for the Mg^{2+} and the Ca^{2+} complexes, respectively. In the first substitution, the aquacomplex is a dication that interacts strongly with a dianion, while in the second substitution the aquacomplex is a neutral specie that interacts with the dianion. In this way, in the first substitution the electrostatic stabilization energy is larger (interaction of two charged moieties) than in the second substitution (interaction of a neutral and a charged molecule), leading to more negative interaction enthalpy values.

Table 1 also shows that for the first ligand substitution the interaction of the ligands with Mg^{2+} is 5.97 ± 2.40 kcal mol^{-1} stronger than with Ca^{2+}. This is related to the electrostatic

Table 1. Optimized geometry of the mono- and disubstituted aquacations (Geo), interaction enthalpy (ΔH), Gibbs free energy (ΔG) and entropic component (–TΔS) at 298 K, for the water exchange by one (monosubstituted complexes) or two ligands (disubstituted complexes) molecules

Ligand	Mg^{2+}				Ca^{2+}			
	Geometry[a]	ΔH[b] / (kcal mol^{-1})	ΔG[b] / (kcal mol^{-1})	–TΔS / (kcal mol^{-1})	Geometry[a]	ΔH[b] / (kcal mol^{-1})	ΔG[b] / (kcal mol^{-1})	–TΔS / (kcal mol^{-1})
Monosubstituted complexes								
tdt	Oh	–339.92	–349.25	–9.33	Oh	–336.38	–335.06	1.32
bdt	Oh	–341.52	–349.05	–7.53	Oh	–336.10	–334.54	1.56
Cl_2-bdt	Oh	–322.82	–334.10	–11.28	Oh	–318.65	–318.19	0.46
edt	Oh	–355,44	–362.53	–7.09	Oh	–350.28	–348.57	1.71
mdt	Oh	–354.61	–361.49	–6.88	Oh	–349.49	–347.91	1.58
tfd	Oh	–320.08	–327.71	–7.63	Oh	–312.08	–312.27	–0.19
mnt	Oh	–308.70	–313.30	–4.60	Oh	–298.30	–298.32	–0.02
Disubstituted complexes								
$(tdt)_2$	Td	–39.55	–48.64	–9.09	Oh	–45.61	–53.86	–8.25
$(bdt)_2$	Td	–41.75	–51.56	–9.81	Oh	–60.65	–68.57	–7.92
$(Cl_2\text{-}bdt)_2$	Oh	–36.96	–42.83	–5.87	Bp	–55.53	–62.39	–6.86
$(edt)_2$	Td	–44.47	–53.42	–8.95	Td	–43.79	–53.65	–9.86
$(mdt)_2$	Bp	–44.94	–50.94	–6.00	Bp	–46.08	–53.36	–7.28
$(tfd)_2$	Oh	–46.05	–51.96	–5.91	Oh	–57.86	–64.55	–6.69
$(mnt)_2$	Oh	–44.66	–51.38	–6.72	Oh	–59.13	–66.29	–7.16

[a]Oh: octahedral; Bp: bipyramidal; Td: tetrahedral; [b]including the BSSE correction (Table S1, in Supplementary Information section); tdt: toluene-3,4-dithiolate; bdt: benzene-1,2-dithiolate; Cl_2-bdt: 3,6-dichlorobenzene-1,2-dithiolate; edt: ethylene-1,2-dithiolate; mdt: 1,2-dimethyl-1,2-ethylenedithiolate; tfd: bis(trifluoromethyl) ethylenedithiolate; mnt: maleonitrile-2,3-dithiolate.

stabilization energy of the interaction. As this bond is formed by a cation and an anion, the size of each specie must be strictly related with its strength. As Mg^{2+} has a smaller ionic radius than Ca^{2+}, its electrostatic stabilization energy is higher, leading to more negative interaction enthalpies and larger affinity.

In the second substitution by the dithiolene ligand, the trend is the opposite seen for the first substitution. Almost all ligands have larger affinity for the Ca^{2+} cation, 11.83 ± 7.85 kcal mol^{-1} stronger than with the Mg^{2+} cation. As the ionic radius of the Ca^{2+} cation is larger than the Mg^{2+}, it can be more stabilized by orbital overlap with the ligands, indicating stronger covalent character. Only the edt ligand presented larger affinity for the Mg^{2+} cation of 0.88 kcal mol^{-1}, that may be related to its structure, as it is the only molecule that complex in a tetrahedral arrangement with both cations.

The analysis of the interaction enthalpy change can be done by comparing the values for the tdt and mnt ligands, which are in the extremes. The first and the second ligand substitution have the same trend for both metal cations. The ΔH for the first substitution varies 31.22 and 38.08 kcal mol^{-1} for the Mg^{2+} and Ca^{2+} cations, respectively. Whereas for the second substitution the ΔH varies 9.09 and 16.86 kcal mol^{-1} for the Mg^{2+} and Ca^{2+} complexes, respectively. We observe that the ΔH is larger for the first substitution than for the second substitution. This must be related to the charges on the metallic center of the complexes. In the first substitution, the charges on the metal cations are more positive than the ones in the second substitution. This enhances the affinity of the ligand by the cation and justifies the homogeneity of the results on the second ligand substitution.

The analysis of the interaction enthalpy of each ligand for Mg^{2+} and Ca^{2+} shows similar behaviors that can be rationalized based on the resonance and induction electronic effects inherent to each ligand substituent. The ΔH values are negative showing the preference of the metal cation to coordinate with the dithiolene ligands instead of with water molecules. As previously shown in Figure 1, there are two types of ligands: the double bond, containing the ethylenic disulfide functional group (Figures 1a-1c) and the aromatic ligands (Figures 1d-1g). In the first substitution of the aromatic series we note that the tdt and bdt ligands have similar affinity for the Mg^{2+} (1.60 kcal mol^{-1}) and the Ca^{2+} (0.28 kcal mol^{-1}) cations. This is probably due to the weak electron donation effect of the methyl group promoting a small enhancement of the charge on the ligand's interacting atom. The Cl_2-bdt ligand has the most positive ΔH values of this series, showing the weakest

interaction. The metal interaction with the Cl_2-bdt ligand is 18.70 and 17.45 kcal mol^{-1} weaker than with the bdt ligand for the Mg^{2+} and Ca^{2+} cations, respectively. This is due to the inductive effect of the aromatic chloro substituents, that reduces the charge on the benzene ring and consequently on the S atoms, weakening the interaction magnitude. In the second ligand substitution, this trend is maintained for the Mg^{2+} complexes, with the following interacting order bdt > tdt > Cl_2-bdt. However, for the Ca^{2+} complexes this trend is distinct (bdt > Cl_2-bdt > tdt), maybe due to the different coordination spheres. The coordination geometry of the tdt and bdt is octahedral (6 ligand donation sites for the metal) and for the Cl_2-bdt bipyramidal with trigonal base (5 donation sites, where the interaction is strengthened). The reduced coordination number of the metal center for the Cl_2-bdt complex makes the cations more electrophilic, enhancing the interaction strength.

The affinity of the second series of ligands containing the ethylenic disulfide group (Figures 1d-1g) for the metal cations is also modulated by the electronic nature of the substituent on the ligands. In the first ligand substitution, the interaction order strength is edt > mdt > tfd > mnt for both the Mg^{2+} and Ca^{2+} aquacations. The edt and mdt compounds are very similar in structure, differing by two methyl groups. The methyl groups have a weak inductive effect that slightly enhances the negative charge on the ethylene moiety and thus in the coordinating S atoms, strengthening the interaction. The interaction enthalpy difference between the edt and mnt ligands is 0.83 and 0.89 kcal mol^{-1} for the Mg^{2+} and Ca^{2+} complexes, respectively. The two compounds of this series that have the weakest interaction strength are the tfd and mnt, respectively, due to the strong electron acceptor substituents on the C=C bond. The tfd contains 3 F atoms that withdraw electron density from each of the coordinating S atoms by the inductive effect, decreasing the interaction enthalpy by 34.53 and 37.41 kcal mol^{-1} (comparing with the mdt ligand) for the Mg^{2+} and Ca^{2+}, respectively. The mnt has two CN substituents that also withdraw electron density, by the resonance effect, and reduce the interaction enthalpy by 45.91 and 51.19 kcal mol^{-1} (comparing with the mdt ligand) for the Mg^{2+} and Ca^{2+}, respectively. In the mnt ligand the entire π-electron system is conjugated with parallel orbitals, allowing strong electronic acceptance by the CN group, which leads to a less stable aqua complex. In the second ligand substitution, the interaction strength order for the Mg^{2+} complexes is tfd > mdt > mnt > edt > bdt > Cl_2-bdt. For the Ca^{2+} cation the interaction order strength is bdt > mnt > tfd > Cl_2-bdt > mdt > edt. It is interesting to observe that ligands with electron withdrawing groups (tfd, mnt) have the strongest interactions. This is probably due to the amount of negative charge that the Mg^{2+} and Ca^{2+} metal cations can receive to form the interactions. In the second substitution the metal aquacenter is neutral and does not tend to form interactions with predominant electrostatic character, being the covalent term also important to describe the bond. The electronic character analysis of the metal-ligand bond is discussed in the EDA part below.

The analysis of the ΔG values shows similar trends as the enthalpy strength order, for the two series of ligands and for the first and second ligand substitution. All the ΔG values are negative, showing that the substitutions of two and four water molecules by bidentate ligands are both spontaneous processes. The ΔG values are 7.62 ± 1.85 and 3.40 ± 4.57 kcal mol^{-1} more negative than the ΔH values for the Mg^{2+} and Ca^{2+} aquacations, respectively. The analysis of the set of substituents follows similar trends, as for the enthalpy. In the first substitution of the aromatic ligands, the interaction strength order is tdt 0.20 (0.52) kcal mol^{-1} stronger than bdt and 15.15 (16.35) kcal mol^{-1} stronger than Cl_2-bdt for the Mg^{2+} (Ca^{2+}) complexes. The double bond ligands interaction order is: edt 0.83 (0.79) kcal mol^{-1} stronger than mdt 34.53 (37.41) kcal mol^{-1} stronger than tfd and 11.38 (13.78) kcal mol^{-1} stronger than mnt for the Mg^{2+} (Ca^{2+}) aquacomplexes. In the second substitution, the analysis of the interaction of Mg^{2+} with the aromatic ligands shows the following trend bdt (2.92 kcal mol^{-1} more negative than) > tdt (5.81 kcal mol^{-1} more negative than) > Cl_2-bdt. This order is justified by the electronic effects related to the methyl group and Cl atom. For the Ca^{2+} complexes, the interaction order with the aromatic ligands is bdt (6.18 kcal mol^{-1} more negative than) > Cl_2-bdt (8.53 kcal mol^{-1} more negative than) > tdt, due to the change of the coordination geometry. The interaction order of the Ca^{2+} cation with the ethylenic ligands is mnt (1.74 kcal mol^{-1} more negative than) > tfd (10.90 kcal mol^{-1} more negative than) > edt (0.29 kcal mol^{-1} more negative than) > mdt. As previously seen for the enthalpy analysis, the modulation of these interactions is mainly due to the inductive and mesomeric electronic effects inherent to the substituents of the dithiolene ligands. These results are in agreement with the work performed by Ghiasi and Monajjemi[72] in the calculation of the affinity of alkaline earth metal cations with dithiolene ligands (cyclobutene-1,2-dithione-3,4-dithiolate) that also reports the substituent modulation.

Table 1 also shows the values for the entropic (–TΔS) parameter for each complex. All entropic contributions are negative for the first and the second ligand substitutions of the Mg^{2+} complexes. For the Ca^{2+} complexes the (–TΔS) term is negative (second substitution reaction) or nearly zero (first substitution reaction). In the substitutions

reactions (equations 1 and 2), the number of products is larger than the number of reactants, due to the coordination of the metal cation with a bidentate ligand and the release of two water molecules. This confirms the effect of the enhancement of the system disorder as expected for chelate ligands. Specifically, for the first ligand substitution, it is observed that the values for Mg^{2+} complexes are 8.68 ± 2.13 kcal mol^{-1} more negative than those for the Ca^{2+} complexes, while in the second substitution the values are almost the same (0.24 ± 1.08 kcal mol^{-1}).

Chelate effect

The chelate effect arises from the entropic stabilization of complexes with polydentate ligands relative to analogous complexes in which the ligand is monodentate. Ligands that contain more than one anchor point to coordinate with a metal cation form chelate systems. The formation constants for the chelate formation reaction generally have high values due the stabilizing effect of the product. The chelate effect can be explained using the additional stabilization caused by the difficulty to break the complex. In a previous study[73] we quantified the stabilization energy for O-containing bidentate ligands with Ca^{2+}. For dithiolenes, this phenomenon can be quantified in equation 3, by the calculation of half of the ΔH and ΔG values. In this case, we chose to evaluate the structure with bridged dithiolate ligands, considering this specie as a theoretical model. In this way, it was possible to calculate the substitution energy with the edt ligand like monodentate ligand. The results are listed in Table 2.

$$2[Ca(H_2O)_6]^{2+} + L \rightarrow [(Ca(H_2O)_5)_2L] + 2H_2O \quad (3)$$

The entropic contributions in Table 2 are positive, as the number of specie on both sides of equation 3 is the same. The –TΔS term changes from –7.09 (bidentate) to 2.78 (monodentate) and 1.71 (bidentate) to 3.92 kcal mol^{-1} (monodentate), for the Mg^{2+} and Ca^{2+} complexes, respectively, for the first substitution reaction. This shows that the bidentate coordination is substantially more favorable entropically. Also, the results in Table 2 show that the interaction of the edt ligand as a monodentate specie yields less negative ΔH and ΔG than those calculated for the bidentate type of (Table 1).

Table 2. Interaction enthalpy (ΔH), Gibbs free energy (ΔG) and entropic component (–TΔS) at 298 K, for the interaction of the edt ligand (L) with two molecules of the $[M(H_2O)_5]^{2+}$ (M = Mg or Ca) complexes

	ΔH / (kcal mol^{-1})	ΔG / (kcal mol^{-1})	–TΔS / (kcal mol^{-1})
$[(Mg(H_2O)_5)_2L]$	–318.04	–315.26	2.78
$[(Ca(H_2O)_5)_2L]$	–209.39	–205.47	3.92

Energy decomposition analysis (EDA)

This procedure fragments the interaction energy ($E_{Tot.}$) between two moieties in the electrostatic ($E_{Elec.}$), polarization ($E_{Pol.}$), exchange ($E_{XC.}$), dispersion ($E_{Disp.}$) and Pauli repulsion (E_{Pauli}) terms.[49-51] In the complexes, one fragment is the aquacation $[M(H_2O)_4]^{2+}$ or $[M(H_2O)_2L]$ and the other is the ligand L that binds to the aquacation according to equations 1 and 2.

Table 3 shows the EDA results for both the Mg^{2+} and Ca^{2+} aquacomplexes for the first and second ligand substitutions. The total interaction energy orders for the first and second substitutions are the same as these of the substitution enthalpy and Gibbs free energy. Therefore, the electronic nature of each substituent on the ligand molecule modulates this parameter, as discussed in the previous section. The total interaction energy is 112.55 ± 5.34 kcal mol^{-1} (108.96 ± 8.97 kcal mol^{-1}) and 75.02 ± 9.94 kcal mol^{-1} (69.04 ± 9.17 kcal mol^{-1}) more negative than the interaction enthalpy for the first substitution and second ligand substitution, respectively, of the Mg^{2+} (Ca^{2+}) complexes. The metal-ligand interaction in the first ligand substitution is stronger than that in the second substitution because initially the metal is more electrophilic as it is surrounded only by neutral ligands and

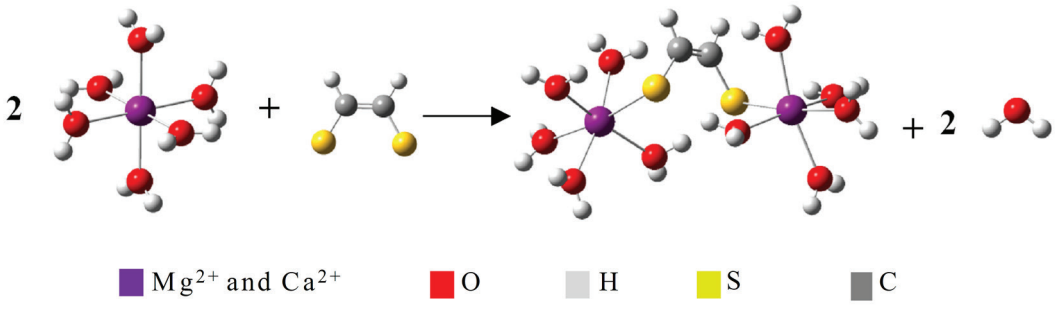

Figure 5. Complexation reaction of $[M(H_2O)_6]^{2+}$ with edt dithiolene ligand (L).

Table 3. Total interaction energy ($E_{Tot.}$), electrostatic ($E_{Elec.}$), polarization ($E_{Pol.}$), exchange ($E_{XC.}$), dispersion (E_{Disp}) and Pauli repulsion (E_{Pauli}) components of the interaction, calculated using the EDA method

Ligand	Mg^{2+}						Ca^{2+}					
	$E_{Tot.}$ / (kcal mol^{-1})	$E_{Elec.}$ / (kcal mol^{-1})	$E_{Pol.}$ / (kcal mol^{-1})	$E_{XC.}$ / (kcal mol^{-1})	$E_{Disp.}$ / (kcal mol^{-1})	E_{Pauli} / (kcal mol^{-1})	$E_{Tot.}$ / (kcal mol^{-1})	$E_{Elec.}$ / (kcal mol^{-1})	$E_{Pol.}$ / (kcal mol^{-1})	$E_{XC.}$ / (kcal mol^{-1})	$E_{Disp.}$ / (kcal mol^{-1})	E_{Pauli} / (kcal mol^{-1})
Monosubstituted complexes $[M(H_2O)_4L]$												
tdt	–453.82	–463.32	–109.26	–49.78	–18.61	168.15	–469.27	–454,57	–109.80	–58.39	–21.36	204.24
bdt	–453.72	–461.21	–107.35	–49.84	–18.62	168.32	–470.68	–454.11	–107.75	–58.68	–21.41	204.42
Cl_2-bdt	–434.35	–444.06	–106.00	–46.41	–17.05	159.76	–441.21	–427.27	–104.48	–53.46	–19.17	191.05
edt	–483.38	–477.34	–98.14	–54.83	–20.22	179.23	–489.76	–467.52	–101.63	–60.84	–23.95	208.66
mdt	–478.03	–480.46	–107.97	–54.67	–20.20	180.41	–494.02	–468.62	–108.67	–65.03	–22.94	222.04
tfd	–435.30	–435.80	–95.51	–45.86	–15.61	156.48	–439.26	–416.16	–92.24	–51.44	–17.39	184.17
mnt	–407.39	–414.67	–93.55	–41.50	–16.04	143.82	–409.43	–394.20	–87.83	–45.75	–17.31	166.12
Disubstituted complexes $[M(H_2O)_2L_2]^{2-}$												
$(tdt)_2$	–156.84	–154.41	–94.81	–58.39	–14.35	165.12	–132.98	–145.81	–63.88	–38.94	–12.34	128.00
$(bdt)_2$	–160.99	–160.93	–96.83	–62.20	–15.97	174.93	–142.27	–158.85	–65.69	–44.21	–13.81	140.29
$(Cl_2\text{-}bdt)_2$	–138.41	–150.68	–81.61	–58.28	–14.60	166.76	–132.12	–144.83	–58.59	–33.50	–11.03	115.84
$(edt)_2$	–161.15	–167.21	–93.71	–66.65	–16.81	183.22	–159.24	–175.88	–68.66	–47.46	–17.05	149.81
$(mdt)_2$	–132.82	–142.80	–85.04	–63.67	–14.61	173.29	–134.86	–151.81	–62.75	–42.44	–12.87	135.01
$(tfd)_2$	–144.43	–159.10	–75.87	–56.38	–14.81	161.73	–146.05	–163.12	–58.80	–38.50	–12.82	127.19
$(mnt)_2$	–135.87	–140.81	–72.15	–46.38	–13.22	136.69	–135.01	–146.41	–55.77	–31.70	–11.33	110.21

Tdt: toluene-3,4-dithiolate; bdt: benzene-1,2-dithiolate; Cl_2-bdt: 3,6-dichlorobenzene-1,2-dithiolate; edt: ethylene-1,2-dithiolate; mdt: 1,2-dimethyl-1,2-ethylenedithiolate; tfd: bis(trifluoromethyl) ethylenedithiolate; mnt: maleonitrile-2,3-dithiolate.

the entire complex is a dication. After the first substitution, the entire complex becomes neutral and the electrophilicity of the metal center is decreased due to the coordination with one anionic dithiolene ligand.

In the first ligand substitution, the electrostatic component of the interaction is the major one, with contribution of 72.81 ± 0.55 and 71.19 ± 0.77% of the total stabilizing terms for the Mg^{2+} and Ca^{2+} complexes, respectively. The metal-S chemical bond in the complexes produced in the first substituted aquacomplexes is predominantly ionic, as noted above. The electronic character of the ligand substituents also modulates the electrostatic term. The complexes containing electron-donating ligand substituents have more negative electrostatic component than those containing electron-withdrawing substituents. The electrostatic component of the Mg^{2+} aquacations is 13.49 ± 5.43 kcal mol^{-1} larger than of the Ca^{2+} complexes for the first ligand substitution.

For the second ligand substitution, we observe two trends. The electrostatic component of the Mg^{2+} complexes containing phenyl dithiolenes is 5.51 ± 3.27 kcal mol^{-1} more negative than that of the Ca^{2+} complexes, with the same interaction order as the monosubstituted complexes. For the ethylenic dithiolenes, the electrostatic component of the Ca^{2+} complexes are 3.90 ± 2.42 kcal mol^{-1} more negative than that of the Mg^{2+} complexes, with a reverse interaction order compared to the monosubstituted complexes. As Mg^{2+} has a smaller ionic radius than Ca^{2+}, it can accommodate a smaller quantity of electron density. As both cations are interacting with two dianionic ligands, in the second substitution the Mg^{2+} complex is more saturated with electron density, while the Ca^{2+} complex can still receive electrons. This behavior enhances the electrostatic component of Ca–S bonding in comparison with the Mg–S bonding in the second ligand substitution.

It is important to consider the electrostatic term in comparison between the first and second dithiolene substitution for the same metal center. The electrostatic terms of the first substitution in the Mg^{2+} and Ca^{2+} complexes are 300.13 ± 21.87 and 285.10 ± 26.26 kcal mol^{-1} more negative, respectively, than these of the second substitution. This is related with the affinity of the aquacenters for the ligands. The first substitution occurs in the $[M(H_2O)_6]^{2+}$ specie, where the cation is surrounded by neutral ligands, whereas the second substitution occurs in the neutral complex $[M(H_2O)_4L]$. In the latter, the metal center has a weaker attraction for the second dithiolene ligand due to the interaction with the first dithiolene that largely neutralized its electronic charge, decreasing its electrophilicity.

In EDA, the covalent character is accounted by the sum of the polarization and exchange terms. The polarization is the main term of the covalent component representing

67.70% (64.46%) and 59.28% (61.21%) of the covalent terms of the first and second dithiolene substitutions, respectively, for the Mg^{2+} (Ca^{2+}) complexes. As seen for the electrostatic term, the polarization component of the first substitution is larger than that of the second substitution by 16.82 ± 7.33 and 39.75 ± 6.63 kcal mol^{-1} for the Mg^{2+} and Ca^{2+} complexes, respectively. Before the first dithiolene substitution, the metal center is only bound to neutral molecules with low orbital overlap. After the first dianion coordination, the metal-ligand distance decreases, enhancing the orbital overlap and leading to increased polarization term values. In the second substitution, besides the metal having a lower electrophilicity that weakens the interaction (and decreases the polarization term), the metal aquacomplex has higher electronic density that repulses the electronic cloud of the second dithiolene ligand, decreasing the coordination strength and lowering the polarization term. The dispersion ($E_{Disp.}$) term is the one with the smallest change, of less than 8 kcal mol^{-1} for both cations. The dispersion terms for the first ligand substitution are 3.14 ± 1.51 and 7.47 ± 1.85 kcal mol^{-1} more negative than for the second substitution in the Mg^{2+} and Ca^{2+} complexes. This is also related to the decrease of the electrophilicity and saturation of the electronic charge of the metal center.

Table 3 also lists the variation of the Pauli repulsion term with each dithiolene ligand. The results show that the Pauli repulsion is larger for the aquacomplexes that have the strongest interaction with the ligands. This is probably due to larger electronic repulsion between the electron density of the ligand and the metal that may be enhanced as the M–S distance is shortened. We also note that the Cl_2-bdt ligand has lower electrostatic and Pauli repulsion term values compared with the other phenyl dithiolene ligands. This is due to the inductive effect of electron density withdrawal discussed above. In the ethylenic dithiolene ligand series, the electronic nature of the substituent reveals the same behavior: the tfd and mnt ligands F and CN substituents have lower Pauli repulsion due to the weaker metal-ligand interaction and longer M–S bonds.

Figure 6 shows a graph of the ionic and covalent terms of the dithiolene coordination, which gives a visual presentation of their magnitudes. The results show that for the monosubstituted $[Mg(H_2O)_4L]$ and $[Ca(H_2O)_4L]$ complexes the principal electronic stabilizing effect is through the electrostatic character. This term stabilizes completely the metal-ligand coordination interaction, demonstrating that electron donating moieties contribute for this interaction. It is noteworthy that the disubstituted $[Ca(H_2O)_2L_2]^{2-}$ and $[Mg(H_2O)_2L_2]^{2-}$ complexes have smaller

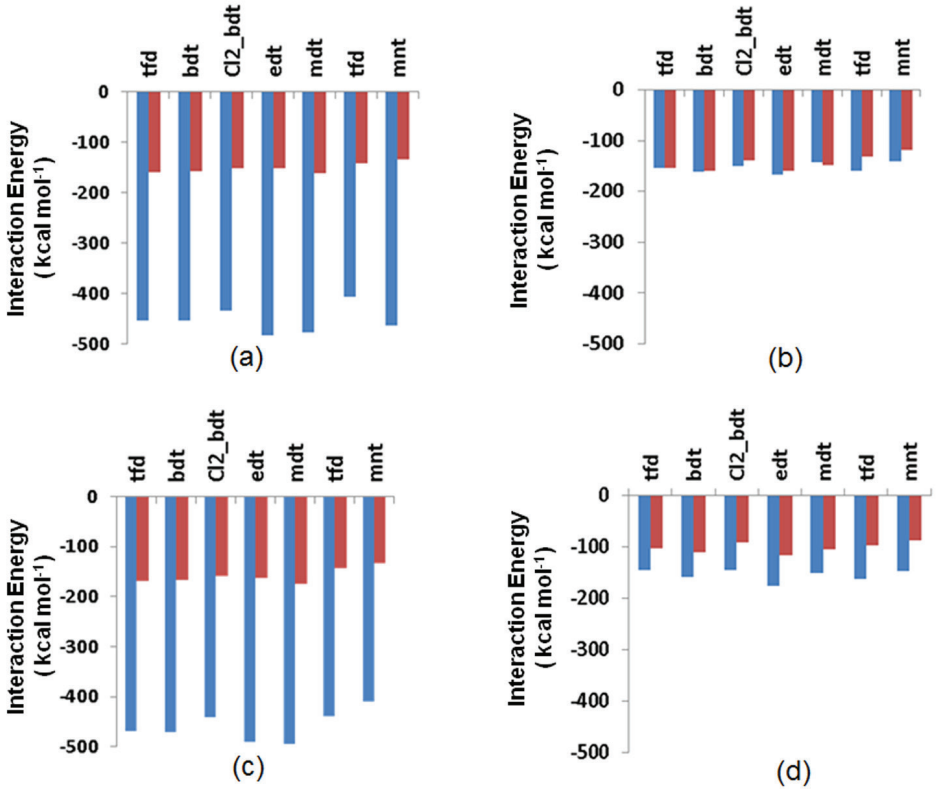

Figure 6. Ionic (blue) and covalent (red) components of the metal-ligand interaction, in kcal mol^{-1}, for the (a) $[Mg(H_2O)_4L]$; (b) $[Mg(H_2O)_2L_2]^{2-}$; (c) $[Ca(H_2O)_4L]$ and (d) $[Ca(H_2O)_2L_2]^{2-}$ complexes.

electrostatic term compared with the monosubstituted complexes. In the evaluation of the second dithiolene substitution, a reduction of the ionic component of 55 to 35% compared to the first dithiolene ligand substitution is evident. This is due to the nature of the interaction of the neutral complexes $[M(H_2O)_4L]$ with the dianionic dithiolene ligands. Even if there were a positive partial charge in the metal center, it will be much lower than in the $[M(H_2O)_6]^{2+}$ aquacomplexes. Coordination is favored by maintaining of the covalent character that gradually becomes relevant, as observed in Figure 3. However, it is evident that for the Mg^{2+} complexes the covalent component is comparable to the ionic term, confirming the relevance of the electron donation effect in this coordination. For the Ca^{2+} complexes, we found the ionic character more dominant in the metal-ligand interaction, with more than 50% contribution to the total metal-ligand interaction energy.

Geometrical, electronic and energetic parameters analysis

We observed that some geometrical (metal-ligand distance and chelation angle), electronic (charge on specific atoms) and energetic (softness) parameters of the complexed aquacations are strictly correlated with the metal-ligand bond strength. As the first metal-ligand substitution has a substantial ionic character, the distance between the charged atoms must be important in the modulation of the bond strength. A bibliographic review in the Cambridge Crystallography Data Centre (CCDC) database[74,75] reveals a few complexes of polydentate ligands coordinating via a S atom with Mg and Ca. We found 13 structures containing Ca^{2+} coordinated with bidentate S chelates and 4 structures with tetradentate S chelates. A search for analogous Mg complexes found 3 Mg chelates with tetradentate S ligands. The bond lengths in the bidentate systems are 2.55-2.66 and 2.74-3.14 Å for Mg–S and Ca–S, respectively. The small number of structures could be associated with the ionic character of the bonds, high solubility in water and in the solid state the weak direct interaction with the metallic ions.[76]

Table 4 lists the metal-ligand bond distances for $[M(H_2O)_4L]$ and $[M(H_2O)_2(L)_2]$ complexes. It is important to note that there is an asymmetry in the Mg–S binding distances in the aquacomplex formed after the first ligand substitution, indicating that one of the dithiolene S atoms interacts stronger than the other. All the M–S distances for the Mg^{2+} complexes are shorter than those of the Ca^{2+} aquacomplexes. As the ligands are the same, the ionic radius of the metal center can justify this effect. As Ca^{2+} has a larger ionic radius than Mg^{2+}, the Ca^{2+} complexes must have longer M–S bonds than the Mg^{2+} aquacomplexes. After the second substitution, the variations of the M–S bond lengths are much smaller, showing more equivalent coordination. This may be related to the steric arrangement

Table 4. Metal-ligand bond distances (D_{M-L1}, D_{M-L2}, D_{M-L3} and D_{M-L4}), of the $[M(H_2O)_4L]$ and $[M(H_2O)_2L_2]^{2-}$ (M = Mg or Ca) complexes

Ligand	$[M(H_2O)_4L]$		$[M(H_2O)_2L_2]^{2-}$			
	D_{M-L1} / Å	D_{M-L2} / Å	D_{M-L1} / Å	D_{M-L2} / Å	D_{M-L3} / Å	D_{M-L4} / Å
			Mg^{2+}			
tdt	2.411	2.498	2.449	2.468	2.482	2.501
bdt	2.411	2.506	2.477	2.477	2.483	2.484
Cl_2-bdt	2.407	2.487	2.544	2.544	2.545	2.546
edt	2.434	2.513	2.501	2.501	2.514	2.514
mdt	2.423	2.470	2.478	2.550	2.598	2.630
tfd	2.411	2.498	2.553	2.554	2.554	2.555
mnt	2.440	2.513	2.528	2.593	2.613	2.640
			Ca^{2+}			
$(tdt)_2$	2.731	2.732	2.777	2.850	2.854	2.913
$(bdt)_2$	2.734	2.734	2.837	2.837	2.846	2.846
$(Cl_2\text{-bdt})_2$	2.741	2.741	2.747	2.802	2.814	2.832
$(edt)_2$	2.721	2.722	2.765	2.765	2.772	2.722
$(mdt)_2$	2.722	2.722	2.758	2.826	2.834	2.847
$(tfd)_2$	2.740	2.761	2.823	2.825	2.829	2.829
$(mnt)_2$	2.749	2.793	2.415	2.798	2.866	2.866

Tdt: toluene-3,4-dithiolate; bdt: benzene-1,2-dithiolate; Cl_2-bdt: 3,6-dichlorobenzene-1,2-dithiolate; edt: ethylene-1,2-dithiolate; mdt: 1,2-dimethyl-1,2-ethylenedithiolate; tfd: bis(trifluoromethyl) ethylenedithiolate; mnt: maleonitrile-2,3-dithiolate.

of the hydrogen atoms of the water molecules near the S atoms that could weaken the M–S interactions. In general, the bond lengths correlate with the sizes of the calcium and magnesium ions, where the Mg–S bond lengths are always shorter.

Upon further examination of the results, we observe the influence of the substituent groups on the first ligand substitution reaction. The Mg complexes containing phenyl and ethylenic dithiolenes with electron-withdrawing groups, such as Cl_2-bdt and tfd, have shorter Mg–S distances than those with electron-donating groups. As Cl_2-bdt and tfd molecules have electron withdrawing substituents, they cause the reduction of the electronic repulsion between the ligands and the metal center allowing enhanced metal-ligand coordination. The smaller size of the magnesium aquacenter reduces even more the electronic repulsion,[71] being with the smallest metal-ligand distances. In the Ca^{2+} complexes, we found an inverse trend as the larger metal center can better accommodate the bidentate ligands and will have larger metal-ligand distances.

In the second ligand substitution, we observe an alteration of the coordination sphere with fewer water molecules coordinated in some cases. Thus, in the Mg^{2+} complexes, the phenyl dithiolenes favor tetrahedral geometry with shorter Mg–S distances for tdt and bdt ligands. In the Cl_2-bdt complex, we found longer Mg–S bonds accommodating the octahedral coordination obtained was octahedral. This trend repeated for the ethylenic dithiolene complexes. Shorter bond distances are found in tetra- and pentacoordinated aquacomplexes (edt and mdt, respectively), whereas for the tfd and mnt ligands with inductive electron-withdrawing effect, the octahedral coordination is retained. For the Ca^{2+} complexes, the variations in the coordination sphere followed the trend that less crowded coordination sphere favors a reduction in the bonding distance.

Table 5 lists the chelation angles for the $[M(H_2O)_4(L)]$ and $[M(H_2O)_2L_2]^{2-}$ complexes. As expected through the analysis of the M–S bond lengths in Table 3, we find that the larger S–M–S angles are observed for the Mg^{2+} aquacomplexes. This can be justified due to the large electronic repulsion effect observed in the accommodation of the bulky atoms, such as sulfur. In the case of the Ca^{2+} complexes, the chelation angle values are always smaller than for the Mg^{2+} analogs, regardless of the number of ligands. Evaluation of the chelate angles variation as a function of the number of ligands shows that the angles are probably decreased to accommodate the larger electron density available at the S atoms. The chelate angle variation for the second ligand substitution is associated with the formation of tetrahedral complexes with a smaller number of ligands around the metal ions, as for edt, tdt and bdt ligands. Finally, by evaluating the influence of the ligand substituents we highlight the effect of electron-withdrawing groups, such as Cl and F for Cl_2-bdt and tfd, decreasing the electron density on the S atoms and consequently decreasing the chelation angles.

The analysis of the charge distribution on the aquacomplexes is performed on the metal center to corroborate the observations discussed previously. Table 6 contains the Mulliken charges on the metal atoms. The results indicate that for the first ligands substitution the charge on Ca is twice as large as that on Mg. This may be associated with a larger concentration of charge on the larger Ca, justifying a possible more pronounced ionic character of the Ca–S interactions. This holds in part for the second substitution, where, on average, the charges are decreased for both metals, but with slightly larger values for the Ca center, indicating a probable increase in the covalent character of the metal-ligand interactions.

Lastly, we perform a comparative analysis of the softness of the complexes and ligands evaluated in this work based

Table 5. Chelation angle, upon first and second ligands substitution in the Ca^{2+} and Mg^{2+} complexes

Ligand	$[M(H_2O)_4(L)]$ / degree		$[M(H_2O)_2L_2]^{2-}$ / degree			
	S–Ca–S	S–Mg–S	[a]S_1–Ca–$S_{1'}$	[a]S_2–Ca–$S_{2'}$	[a]S_1–Mg–$S_{1'}$	[a]S_2–Mg–$S_{2'}$
tdt	79.07	90.68	73.77	76.13	86.33	89.07
bdt	78.83	90.23	75.44	75.44	86.93	86.93
Cl_2-bdt	77.18	88.95	75.57	73.50	83.11	83.11
edt	84.93	92.49	82.24	82.24	88.44	88.44
mdt	78.85	90.16	76.62	74.62	83.87	81.79
tfd	76.91	88.30	74.19	74.18	81.77	84.53
mnt	78.86	89.80	76.29	74.53	83.06	80.96

[a]In the disubstituted complexes, the S atoms of each ligand are labeled as S_1, $S_{1'}$ and S_2, $S_{2'}$; tdt: toluene-3,4-dithiolate; bdt: benzene-1,2-dithiolate; Cl_2-bdt: 3,6-dichlorobenzene-1,2-dithiolate; edt: ethylene-1,2-dithiolate; mdt: 1,2-dimethyl-1,2-ethylenedithiolate; tfd: bis(trifluoromethyl) ethylenedithiolate; mnt: maleonitrile-2,3-dithiolate.

Table 6. Mulliken charge, on the metal centers of the aquacomplexes

Ligand	$[M(H_2O)_4(L)]$ / |e|		$[M(H_2O)_2L_2]^{2-}$ / |e|	
	Mg	Ca	Mg	Ca
tdt	0.533	0.898	0.332	0.484
bdt	0.561	0.900	0.249	0.464
Cl_2-bdt	0.451	0.942	0.418	0.574
edt	0.304	0.946	0.438	0.698
mdt	0.248	0.933	0.407	0.566
tfd	0.401	0.960	0.398	0.482
mnt	0.458	0.908	0.452	0.469

Tdt: toluene-3,4-dithiolate; bdt: benzene-1,2-dithiolate; Cl_2-bdt: 3,6-dichlorobenzene-1,2-dithiolate; edt: ethylene-1,2-dithiolate; mdt: 1,2-dimethyl-1,2-ethylenedithiolate; tfd: bis(trifluoromethyl) ethylenedithiolate; mnt: maleonitrile-2,3-dithiolate.

on the HOMO and LUMO energies, as presented in Table 7. Using the interpretation of Pearson,[77,78] we clearly confirm the effect of the expected softness for the dithiolenes with values 4-9 times larger than 2.86 and 2.89 of $[Mg(H_2O)_6]^{2+}$ and $[Ca(H_2O)_6]^{2+}$, respectively. After the substitution of the first dithiolene, we notice a decrease of the softness of the aquacomplexes compared to the pure ligands, evidencing the effect of the presence of the soft ligands on the hard hexaaquacations. In the second substitution, we observed an increase in softness in most cases with a probable effect on the change of the coordination compounds.

Table 7. Softness, σ [σ = 1/(E(LUMO) – E(HOMO)], of the isolated ligands and the Mg^{2+} and Ca^{2+} aquacomplexes

Ligand	L^{2-}	$[M(H_2O)_4(L)]$		$[M(H_2O)_2L_2]^{2-}$	
		Mg^{2+}	Ca^{2+}	Mg^{2+}	Ca^{2+}
tdt	19.23	17.86	15.15	16.67	20.00
bdt	20.00	17.24	14.71	19.23	27.78
Cl_2-bdt	17.24	14.71	12.50	14.29	8.93
edt	13.89	19.23	7.14	33.33	13.16
mdt	26.32	25.00	20.00	27.78	17.24
tfd	13.16	14.29	7.35	17.24	21.74
mnt	11.11	12.50	11.11	11.63	8.20

Tdt: toluene-3,4-dithiolate; bdt: benzene-1,2-dithiolate; Cl_2-bdt: 3,6-dichlorobenzene-1,2-dithiolate; edt: ethylene-1,2-dithiolate; mdt: 1,2-dimethyl-1,2-ethylenedithiolate; tfd: bis(trifluoromethyl) ethylenedithiolate; mnt: maleonitrile-2,3-dithiolate.

Natural bond order NBO analysis

The natural resonance theory (NRT) procedure[52] is employed to evaluate the resonance structures that have large contributions to the final hybrid of each dithiolene ligand. The NRT results are presented in Table 8 and interpreted based on Supplementary Information section (Table S2). The NRT analysis allows the evaluation of the statistical weight of the structures with larger electronic density on the S atoms in the final hybrid structure. In these results, we verify that the edt and mdt ligands have the largest percentage of structures with negative charge on the S atoms, indicating the presence of 3 free electron pairs. These ethylenic ligands have C=C group between the S atoms, which has larger contribution of structures with negative charge on the S atom to the final resonance hybrid than the ligands with the aromatic ring. In the ethylenic dithiolene series, we clearly observe that the presence of electron withdrawing groups (F and CN) decreases the contribution of resonance structures with negative charge on the S atom. This characterizes the coordination sites with two electron pairs and C=S bond. For phenyl dithiolene ligands, the effect of π-relocation increases the participation of structures with C=S bond, compared to the previous case, but significantly increases the relocation of the partial charges on the aromatic ring. In the case of the Cl_2-bdt system, the structures with C=S bond (neutral S atom) contribute the most, evidencing the inductive effect of the Cl atoms.

Table 8. NRT analysis of the sulfur anionic ligands: Percentage contribution of the resonance structures of (S^-)–R–(S^-), (S^-)–$R^{+/-}$–(S^-) and (S^-)–R^-–(S). See Supplementary Information section (Table S1) for details

Ligand[a]	(S^-)–R–(S^-) / %	(S^-)–$R^{+/-}$–(S^-) / %	(S^-)–R^-–(S) / %
tdt	29.58	27.01	24.94
bdt	35.48	19.66	28.74
Cl_2-bdt	27.05	24.30	46.01
edt	75.49	2.90	21.59
mdt	69.66	3.71	23.48
tfd	33.26	5.06	21.55
mnt	44.10	5.50	33.36

[a]The contributions do not total 100% due to the 1% cutoff applied in this analysis; tdt: toluene-3,4-dithiolate; bdt: benzene-1,2-dithiolate; Cl_2-bdt: 3,6-dichlorobenzene-1,2-dithiolate; edt: ethylene-1,2-dithiolate; mdt: 1,2-dimethyl-1,2-ethylenedithiolate; tfd: bis(trifluoromethyl) ethylenedithiolate; mnt: maleonitrile-2,3-dithiolate.

Table 9 lists the second-order perturbation energy results, which represents account for the donor-acceptor interactions between the bonding orbitals (S atoms as the Lewis base) and anti-bonding (metal ion as Lewis acid). The donor-acceptor energies are asymmetric in the first ligand substitution of the Mg^{2+} aquacomplexes. This is justified by the effect of the electrostatic interaction between the H atoms of the water ligands and the S atoms of dithiolenes that weaken the Mg–S coordination, as previously discussed in the previous section. For the Ca^{2+} complexes,

the values of donor-acceptor energy are symmetrical, which is justified by the larger size of the metal center that more effectively accommodates the octahedral coordination geometry. However, the Ca-dithiolene donor-acceptor energy values are much lower than those observed for the respective magnesium aquacomplexes, reflecting the lower covalent character of the Ca–S bonds. The evaluation of the hybrid orbitals of S atoms reveals enhanced p character in the orbital contributing to M–L bonding, where the metal center participates mainly with the s orbital. Specifically for the magnesium aquacomplexes, the hybrid orbitals also indicate low s-orbital participation in the hybridization. Evaluation of the second substitution confirms the enhancement of the covalent character of the Ca–S bonds, with twice large donor-acceptor energy values compared to the monosubstituted complexes. The donor-acceptor energy

Table 9. Donor-acceptor energy (E_{D-A}) and s, p and d character of the metal-ligand bonding orbital

Ligand (L)		E_{D-A} / (kcal mol^{-1})	s / %	p / %	d / %	E_{D-A} / (kcal mol^{-1})	s / %	p / %	d / %
			$[Mg(H_2O)_4L]$				$[Ca(H_2O)_4L]$		
tdt	S_1[a]	69.15	10.51	89.35		11.37	3.32	96.62	
	$S_{1'}$	43.23	7.38	92.52		11.44	3.45	96.49	
	M		98.56	1.30	0.14		92.76	1.43	5.81
bdt	S_1	69.09	10.54	89.31		11.36	3.33	96.61	
	$S_{1'}$	52.33	9.59	90.29		11.36	3.29	96.64	
	M		98.53	1.34	0.13		92.77	1.43	5.80
Cl_2-bdt	S_1	67.06	13.87	86.02		12.53	3.10	96.83	
	$S_{1'}$	56.12	7.60	92.26		13.59	3.74	96.19	
	M		98.55	1.33	0.12		94.20	1.43	5.80
edt	S_1	61.94	8.36	91.51		9.38	3.10	96.84	
	$S_{1'}$	47.72	8.09	91.80		9.39	3.06	96.87	
	M		98.31	1.52	0.17		92.76	1.41	5.83
mdt	S_1	45.63	5.19	94.68		11.21	3.44	96.50	
	$S_{1'}$	22.73	3.13	96.80		11.22	3.45	96.49	
	M		98.62	1.24	0.14		92.42	1.41	5.83
tfd	S_1	40.95	3.03	96.86		13.58	2.47	97.44	
	$S_{1'}$	55.22	7.25	92.61		11.05	3.41	96.51	
	M		98.45	1.41	0.14		94.47	0.93	4.60
mnt	S_1	64.46	11.70	88.19		11.93	1.46	98.45	
	$S_{1'}$	54.26	5.12	94.72		13.10	2.34	97.53	
	M		98.31	1.51	0.17		95.05	0.85	4.11
			$[Mg(H_2O)_2L_2]^{2-}$				$[Ca(H_2O)_2L_2]^{2-}$		
tdt	S_1	27.72	5.62	96.65		20.72	12.49	87.48	
	$S_{1'}$	49.33	9.74	90.16		22.50	7.41	92.52	
	S_2	41.69	10.16	99.27		19.69	68.47	31.51	
	$S_{2'}$	52.43	14.72	85.20		28.26	8.52	91.41	
	M		99.75	0.01	0.24		97.09	0.05	2.86
bdt	S_1	49.72	9.70	90.19		30.98	15.70	84.23	
	$S_{1'}$	49.32	9.71	90.19		30.73	16.09	83.83	
	S_2	49.33	9.71	90.19		30.73	16.09	83.83	
	$S_{2'}$	49.72	9.69	90.20		30.98	15.70	84.22	
	M		99.73	0.01	0.25		98.09	0.02	1.90
Cl_2-bdt	S_1	49.00	9.15	90.75		26.27	12.58	87.35	
	$S_{1'}$	50.16	9.23	90.67		26.65	12.96	86.96	
	S_2	50.18	9.24	90.66		30.29	13.81	86.10	
	$S_{2'}$	48.96	9.14	90.76		26.06	11.48	88.44	
	M		99.58	0.09	0.33		97.26	0.10	2.64
edt	S_1	36.73	7.24	94.74		12.04	77.31	94.79	
	$S_{1'}$	33.88	7.78	95.40		13.62	77.07	98.11	
	S_2	36.67	7.27	94.76		12.04	77.31	98.13	
	$S_{2'}$	33.92	7.76	95.38		13.61	77.07	98.11	
	M		99.78	0.01	0.21		98.06	0.16	1.78

Table 9. Donor-acceptor energy (E_{D-A}) and s, p and d character of the metal-ligand bonding orbital (cont.)

Ligand (L)		E_{D-A} / (kcal mol^{-1})	s / %	p / %	d / %	E_{D-A} / (kcal mol^{-1})	s / %	p / %	d / %
		$[Mg(H_2O)_2L_2]^{2-}$				$[Ca(H_2O)_2L_2]^{2-}$			
mdt	S_1	40.26	9.00	90.92		20.16	71.30	28.68	
	S_1	43.38	9.72	90.20		22.35	7.26	92.68	
	S_2	26.17	7.34	98.12		19.23	10.11	89.85	
	$S_{2'}$	53.12	16.55	83.39		26.15	12.53	87.43	
	M		99.56	0.13	0.32		96.31	0.10	0.04
tfd	S_1	55.92	8.70	91.04		23.54	3.92	95.99	
	$S_{1'}$	45.79	8.45	91.45		20.99	4.94	94.97	
	S_2	43.97	8.40	91.51		22.32	4.80	95.12	
	$S_{2'}$	49.62	7.30	92.59		22.17	74.00	25.97	
	M		99.52	0.11	0.36		96.93	0.02	3.05
mnt	S_1	24.00	2.14	98.00		17.09	74.45	98.25	
	$S_{1'}$	41.11	3.96	95.91		15.75	75.26	99.38	
	S_2	48.80	5.41	94.45		26.65	74.12	97.22	
	$S_{2'}$	30.87	3.08	97.56		12.29	73.88	99.13	
	M		99.41	0.24	0.35		96.98	0.05	2.97

[a]The S_1 and $S_{1'}$ parameters refer to the two S atoms of the monodentate ligand in the monosubstitution case. In the disubstitution case the S_2 and $S_{2'}$ parameters refer to the S atoms of the second monodentate ligand; the M parameter refers to the metal ion (Mg or Ca); tdt: toluene-3,4-dithiolate; bdt: benzene-1,2-dithiolate; Cl_2-bdt: 3,6-dichlorobenzene-1,2-dithiolate; edt: ethylene-1,2-dithiolate; mdt: 1,2-dimethyl-1,2-ethylenedithiolate; tfd: bis(trifluoromethyl) ethylenedithiolate; mnt: maleonitrile-2,3-dithiolate.

remains in the same range for the magnesium mono- and disubstituted complexes. The geometry variations already discussed are also reflected in the hybridization results, with the participation of more than one S atom electron pairs with high p%.

Conclusions

The ability of bidentate ethylenic and phenyl dithiolene ligands to substitute water in the $[Ca(H_2O)_6]^{2+}$ and $[Mg(H_2O)_6]^{2+}$ in two substitution reaction steps is evaluated in terms of energetic and geometric parameters. Generally, the ethylenic dithiolene complexes have more negative enthalpy and Gibbs free energy values than the respective phenyl dithiolene complexes. The interaction enthalpy increase for ethylenic dithiolenes: mnt < tfd < edt < mdt for both Mg^{2+} and Ca^{2+} cations and for phenyl dithiolenes: Cl_2-bdt < tdt < bdt for Mg^{2+} and Cl_2-bdt < bdt < tdt for the Ca^{2+} cation. These orders are mainly determined by the electronic nature of the functional group. The optimized structures of the complexes have coordination numbers of 4 (tetrahedral), 5 (bipyramidal with trigonal base) and 6 (octahedral).

The EDA results show that dithiolene modulates the electrostatic contribution of the interaction stronger than the covalent term. The EDA method shows that the differences in the ability of the ligands to coordinate to the metal center are mainly reflected in the electrostatic component of the interaction energy, which is the major term for the first ligand substitution. In the second ligand substitution, the covalent term becomes as important as the ionic component for the stabilization of the complex. The exchange and dispersion components are almost constant for the series of ligands analyzed, while the Pauli repulsion varies within about one fourth of the variation range of the electrostatic interaction term. The metal-ligand bond lengths, chelation angles, charge on the metal center and the softness of the aquacomplexes are strictly correlated with the of metal-ligand coordination strength.

The NBO results indicate that the steric and electron-withdrawing effects of the atoms adjacent to the metal-ligand coordination modulate the bonding strength of the complexes as well as that the geometric parameters are in a good agreement with the NBO analysis. The donor-acceptor energy of the monosubstituted Mg^{2+} complexes is larger than that of the respective Ca^{2+} complexes, showing increased covalent stabilization. In the second substitution, this trend is maintained, but with a lower magnitude. The evaluation of the hybrid orbitals of S atoms reveals enhanced p character in the orbital contributing to M–L bonding, where the metal the metal center participates mainly with the s orbital. The computational results presented here are important for the rational design of dithiolene complexes for a wide range of advanced applications.

For all the complexes analyzed, the p character of the metal-ligand interacting orbital is the predominant. The computational results presented here are important for the rational design of dithiolene complexes for a wide range of

advanced applications, as previously shown. Additionally, experimental results show that alkaline earth complexes are known as being purely ionic. In this study we show that complexes of alkaline earth metal cations are also stabilized by covalent interactions, as seen in the second ligand substitution for the dithiolene ligands.

Supplementary Information

Supplementary data (BSSE, NRT and cartesian coordinate data) are available free of charge at http://jbcs.sbq.org.br as PDF file.

Acknowledgments

Dr Glaucio Braga Ferreira and Dr Leonardo Moreira da Costa acknowledge FAPERJ (Fundação de Amparo a Pesquisa do Estado do Rio de Janeiro), CNPq (Conselho Nacional de Desenvolvimento Científico e Tecnológico). The authors also thank LQC-UFF for the computational structure provided. Dr S. R. Stoyanov thanks Dr John M. Villegas for discussions. The computations are performed on the high-performance computing resources provided by Compute/Calcul Canada.

References

1. Kato, K.; *Chem. Rev.* **2004**, *104*, 5319.
2. Anthopoulos, T. D.; Setayesh, S.; Smits, E.; Cölle, M.; Cantatore, E.; de Boer, B.; Blom, P. W. M.; de Leeuw, D. M.; *Adv. Mater.* **2006**, *18*, 1900.
3. Bushnell, E. A. C.; Boyd, R. J.; *J. Phys. Chem. A* **2015**, *119*, 911.
4 Stipdonk, M. J.; Basu, P.; Dille, S. A.; Gibson, J. K.; Berden, G.; Oomens, J.; *J. Phys. Chem. A* **2014**, *118*, 5407.
5. Beswick, C. L. J.; Schulman, M.; Stiefel, E. I. In *Dithiolene Chemistry: Synthesis, Properties, and Applications*, vol. 52; Stiefel, E. I., ed.; John Wiley & Sons: Hoboken, USA, 2003.
6. Qi, Y.; Sajoto, T.; Barlow, S.; Kim, E.-G.; Bredas, J.-L.; Marder, S. R.; Kahn, A.; *J. Am. Chem. Soc.* **2009**, *131*, 12530.
7. Qing, D.; Feng, C. X.; Hong, C.; Xing, G.; Ping, Z. X.; Zhusheng, C.; *Supramol. Sci.* **1998**, *5*, 531.
8. Mueller-Westerhoff, U. T.; Vance, B.; Yoon, D. I.; *Tetrahedron* **1991**, *47*, 909.
9. Marshall, K. L.; Painter, G.; Lotito, K.; Noto, A. G.; Chang, P.; *Mol. Cryst. Liq. Cryst.* **2006**, *454*, 449.
10. Curreli, S.; Deplano, P.; Faulmann, C.; Ienco, A.; Mealli, C.; Mercuri, M. L.; Pilia, L.; Pintus, G.; Serpe, A.; Trogu, E. F.; *Inorg. Chem.* **2004**, *43*, 5069.
11. Fan, Y.; Hall, M. B.; *J. Am. Chem. Soc.* **2002**, *124*, 12076.
12. Harrison, D. J.; Nguyen, N.; Lough, A. J.; Fekl, U.; *J. Am. Chem. Soc.* **2006**, *128*, 11026.
13. Romão, M. J.; *Dalton Trans.* **2009**, 4053.
14. Cummings, S. D.; Eisenberg, R.; *Prog. Inorg. Chem.* **2003**, *52*, 315.
15. Shibahara, T.; Tsuboi, M.; Nakaoka, S.; Ide, Y.; *Inorg. Chem.* **2003**, *42*, 935.
16. Helton, M. E.; Gebhart, N. L.; Davies, E. S.; McMaster, J.; Garner, C. D.; Kirk, M. L.; *J. Am. Chem. Soc.* **2001**, *123*, 10389.
17. Zuleta, J. A.; Bevilacqua, J. M.; Eisenberg, R.; *Coord. Chem. Rev.* **1991**, *111*, 237.
18. Fourmigué, M.; *Coord. Chem. Rev.* **1998**, *178*, 823.
19. Papavassiliou, G. C.; Anyfantis, G. C.; Mousdis, G. A.; *Crystals* **2012**, *2*, 762.
20. Eisenberg, R.; Gray, H. B.; *Inorg. Chem.* **2011**, *50*, 9741.
21. Papavassiliou, G. C.; Anyfantis, G. C.; Mousdis, G. A.; *Crystals* **2012**, *2*, 762.
22. Islam, N.; Chimni, S. S.; *J. Mol. Struct.* **2017**, *1130*, 781.
23. Huang, P.; Wang, C.; Chai, Z.; Shi, W.; *Inorg. Chimica Acta* **2017**, *463*, 20.
24. Wolf, C.; Hummel, H.; *J. Chem. Soc., Dalton Trans.* **1986**, 43.
25. Beck, J.; Ben-Amer, Y.; *Z. Anorg. Allg. Chem.* **2007**, *633*, 435.
26. Beck, J.; Ben-Amer, Y.; *Z. Anorg. Allg. Chem.* **2008**, *634*, 1522.
27. Drzewiecka-Antonik, A.; Ferenc, W.; Wolska, A.; Klepka, M. T.; Cristóvão, C.; Sarzynki, J.; Rejmak, P.; Osypiuk, D.; *Chem. Phys. Lett.* **2017**, *667*, 192.
28. Xia, Y.; Miao, Z.; Wang, F.; Yao, H.; Cui, M.; Ma, Y.; Qi, Z.; Sun, Y.; *J. Organomet. Chem.* **2015**, *779*, 81.
29. Plazinski, W.; Drach, M.; *J. Phys. Chem. B* **2013**, *117*, 12105.
30. Tavasoli, E.; Fatahi, A.; *J. Theor. Comput. Chem.* **2009**, *3*, 347.
31. Corral, I.; Mo, O.; Yanez, M.; Scott, A.; Radom, L.; *J. Phys. Chem. A* **2003**, *107*, 10456.
32. Corral, I.; Mó, O.; Yánez, M.; Salpin, J.; Tortojada, J.; Moran, D.; Radom, L.; *Chem.-Eur. J.* **2006**, *12*, 6787.
33. Corral, I.; Mó, O.; Yánez, M.; Salpin, J.; Tortojada, J.; Radom, L.; *J. Phys. Chem. A* **2004**, *108*, 10080.
34. Trujillo, C.; Lamshabi, A. M.; Mó, O.; Yánez, M.; *Phys. Chem. Chem. Phys.* **2008**, *10*, 3229.
35. Pesonen, H.; Aksela, R.; Lassonen, K.; *J. Phys. Chem. A* **2010**, *114*, 466.
36. Despotovic, I.; *New J. Chem.* **2015**, *39*, 6151.
37. Kowalsak-Baron, A.; *Comput. Theor. Chem.* **2015**, *1057*, 7.
38. Quattrociocchi, D. G. S.; Ferreira, G. B.; da Costa, L. M.; Carneiro, J. W. M.; *Comput. Theor. Chem.* **2016**, *1075*, 104.
39. Meuser, M. V. M.; Quattrociocchi, D. G. S.; Costa, L. M.; Ferreira, G. B.; Carneiro, J. W. M.; *Polyhedron* **2015**, *102*, 193.
40. Costa, L. M.; Stoyanov, S. R.; Damasceno, R. N.; Carneiro, J. W. M.; *Int. J. Quantum Chem.* **2013**, *113*, 2621.
41. Costa, L. M.; Ferreira, G. B.; Carneiro, J. W. M.; *J. Mol. Model.* **2013**, *19*, 2669.
42. da Costa, L. M.; Paes, L. W. C.; Carneiro, J. W. M.; *J. Braz. Chem. Soc.* **2012**, *23*, 648.

43. Costa, L. M.; Stoyanov, S. R.; Carneiro, J. W. M.; *J. Mol. Model.* **2012**, *18*, 4389.
44. da Costa, L. M.; Amorim, R. M.; de Macedo Cruz, M. T.; Carneiro, J. W. M.; *Comput. Theor. Chem.* **2012**, *999*, 7.
45. Costa, L. M.; Carneiro, J. W. M.; Paes, L. W. C.; Romeiro, G. A.; *J. Mol. Model.* **2011**, *17*, 243.
46. Costa, L. M.; Carneiro, J. W. M.; Paes, L. W. C.; *J. Mol. Model.* **2011**, *17*, 2061.
47. Costa, L. M.; Carneiro, J. W. M.; Paes, L. W. C.; Romeiro, G. A.; *J. Mol. Struct.: THEOCHEM* **2009**, *911*, 46.
48. Becke. A. D.; *J. Chem. Phys.* **1992**, *96*, 2155.
49. Morokuma, K.; *J. Chem. Phys.* **1971**, *55*, 1236.
50. Morokuma, K.; *Acc. Chem. Res.* **1977**, *10*, 294.
51. Ziegler, T.; Rauk, A.; *Theor. Chim. Acta* **1977**, *46*, 1.
52. Glendening, E. D.; Badenhoop, J. K.; Reed, A. E.; Carpenter, J. E.; Bohmann, J. A.; Morales, C. M.; Landis, C. R.; Weinhold, F.; *NBO 6.0.*; Theoretical Chemistry Institute, University of Wisconsin, Madison, 2013.
53. Becke, A. D.; *J. Chem. Phys.* **1992**, *96*, 2155.
54. McLean, A. D.; Chandler, G. S.; *J. Chem. Phys.* **1980**, *72*, 5639.
55. Blaudeau, J.-P.; McGrath, M. P.; Curtiss, L. A.; Radom, L.; *J. Chem. Phys.* **1997**, *107*, 5016.
56. Clark, T.; Chandrasekhar, J.; Spitznagel, G. W.; Schleyer, P. V. R.; *J. Comput. Chem.* **1983**, *4*, 294.
57. Frisch, M. J.; Pople, J. A.; Binkley, J. S.; *J. Chem. Phys.* **1984**, *80*, 3265.
58. Frisch, M. J.; Trucks, G. W.; Schlegel, H. B.; Scuseria, G. E.; Robb, M. A.; Cheeseman, J. R.; Scalmani, G.; Barone, V.; Mennucci, B.; Petersson, G. A.; Nakatsuji, H.; Caricato, M.; Li, X.; Hratchian, H. P.; Izmaylov, A. F.; Bloino, J.; Zheng, G.; Sonnenberg, J. L.; Hada, M.; Ehara, M.; Toyota, K.; Fukuda, R.; Hasegawa, J.; Ishida, M.; Nakajima, T.; Honda, Y.; Kitao, O.; Nakai, H.; Vreven, T.; Montgomery Jr., J. A.; Peralta, J. E.; Ogliaro, F.; Bearpark, M.; Heyd, J. J.; Brothers, E.; Kudin, K. N.; Staroverov, V. N.; Kobayashi, R.; Normand, J.; Raghavachari, K.; Rendell, A.; Burant, J. C.; Iyengar, S. S.; Tomasi, J.; Cossi, M.; Rega, N.; Millam, J. M.; Klene, M.; Knox, J. E.; Cross, J. B.; Bakken, V.; Adamo, C.; Jaramillo, J.; Gomperts, R.; Stratmann, R. E.; Yazyev, O.; Austin, A. J.; Cammi, R.; Pomelli, C.; Ochterski, J. W.; Martin, R. L.; Morokuma, K.; Zakrzewski, V. G.; Voth, G. A.; Salvador, P.; Dannenberg, J. J.; Dapprich, S.; Daniels, A. D.; Farkas, Ö.; Foresman, J. B.; Ortiz, J. V.; Cioslowski, J.; Fox, D. J.; *Gaussian 09*, *Revision E.01*, Gaussian, Inc., Wallingford CT, 2009.
59. Boys, S. F.; Bernardi, F.; *Mol. Phys.* **1970**, *19*, 553.
60. Simon, S.; Duran, M.; Dannenberg, J. J.; *J. Chem. Phys.* **1996**, *105*, 11024.
61. Trujillo, C.; Lamsabhi, A. M.; Mó, O.; Yánez, M.; Salpin, J.; *Org. Biomol. Chem.* **2008**, *6*, 3695.
62. Peschke, M.; Blades, A. T.; Kebarle, P.; *J. Am. Chem. Soc.* **2000**, *122*, 10440.
63. Schmidt, M. W.; Baldridge, K. K.; Boatz, J. A.; Elbert, S. T.; Gordon, M. S.; Jensen, J. H.; Koseki, S.; Matsunaga, N.; Nguyen, K. A.; Su, S.; Windus, T. L.; Dupious, M.; Montgomery, J. A.; *J. Comput. Chem.* **1993**, *14*, 1347.
64. Gordon, M. S.; Schmidt, M. W. In *Theory and Applications of Computational Chemistry: The First Forty Years*; Dykstra, C. E.; Frenking, G.; Kim, K. S.; Scuseria, G. E., eds.; Elsevier: Amsterdam, 2005, p. 1167.
65. Granovsky, A. A.; *Firefly Version 8*, http://classic.chem.msu.su/gran/firefly/index.html, accessed in November 2017.
66. Schmidt, M. W.; Baldridge, K. K.; Boatz, J. A.; Elbert, S. T.; Gordon, M. S.; Jensen, J. H.; Koseki, S.; Matsunaga, N.; Nguyen, K. A.; Su, S.; Windus, T. L.; Dupuis, M.; Montgomery, J. A.; *J. Comput. Chem.* **1993**, *14*, 1347.
67. Szafran, M.; Komasa, A.; Bartoszak, E.; *J. Mol. Struct.* **2007**, *827*, 101.
68. Dennington, R.; Keith, T. A.; Millam, J. M.; *GaussView*, version 6, Semichem Inc., Shawnee Mission, KS, 2009.
69. Rao, J. S.; Dinadayalane, T. C.; Leszczynski, J.; Sastry, G. N.; *J. Phys. Chem. A* **2008**, *112*, 12944;
70. Tunell, I.; Lim, C.; *Inorg. Chem.* **2006**, *45*, 4811.
71. Huheey, J. E.; Keiter, E. A.; Keiter, R. L.; *Inorganic Chemistry: Principles of Structure and Reactivity*, 4th ed.; Harper Collins College Publisher: New York, 1993, p. 1052.
72. Ghiasi, R.; Monajjemi, M.; *J. Sulfur Chem.* **2007**, *28*, 537.
73. Quattrociocchi, D. G. S.; Meuser, M. V. M.; Ferreira, G. B.; Carneiro, J. W. M.; Stoyanov, S. R.; da Costa, L. M.; *J. Mol. Model*. **2017**, *23*, 60.
74. Fuller, R. O.; Koutsantonis, G. A.; Lozic, I.; Ogden, M. I.; Skelton, B. W.; *Dalton Trans.* **2015**, *44*, 2132.
75. Bilyk, A.; Dunlop, J. W.; Fuller, R. O.; Hall, A. K.; Harrowfield, J. M.; Hosseini, M. W.; Koutsantonis, G. A.; Murray, I. W.; Skelton, B. W.; Stamps, R. L.; White, A. H.; *Eur. J. Inorg. Chem.* **2010**, 2106.
76. Karlin, K. D.; *Frontmatter, Progress in Inorganic Chemistry*, vol. 53; John Wiley & Sons, Inc.: Hoboken, NJ, USA, 2005.
77. Pearson, R. G.; *J. Am. Chem. Soc.* **1963**, *85*, 3533.
78. Pearson, R. G.; *Science* **1966**, *151*, 172.

Submitted: September 3, 2017
Published online: November 27, 2017